Materials Research. 2025; 25(suppl. 1): e20250058
DOI: https://doi.org/10.1590/1980-5373-MR-2025-0058

Hybrid Polyamide Microporous Membranes Obtained with Different Solvents

Airan Magalhães Moura[a], *Joana Suelânia da Silva Lima*[b], *Natália Fernanda Santos Silva*[a], *Joanne Graziela Andrade Mendes*[a], *Carlos Antônio Pereira de Lima*[b], *Keila Machado de Medeiros*[a*]

[a]*Universidade Federal do Recôncavo da Bahia, Centro de Ciência e Tecnologia em Energia e Sustentabilidade, Feira de Santana, BA, Brasil.*
[b]*Universidade Estadual da Paraíba, Departamento de Engenharia Sanitária e Ambiental, Campina Grande, PB, Brasil.*

Received: January 9, 2025; Revised: May 12, 2025; Accepted: July 3, 2025

This research explored a new approach that uses a waste material, polyamide 66 (PA66), as a raw material in the manufacture of membranes for the treatment of textile effluents. Membranes were produced by combining PA66 with silicon carbide (SiC) using the phase inversion technique, in the presence of magnesium chloride, using different solvents such as formic acid and hydrochloric acid. The SiC was characterized using X-ray diffraction and the grain size of the sample was measured. The membranes were characterized using various techniques, including water absorption, porosity, bubble point, average pore radius, contact angle, chemical resistance, water flow and effluent flow. The water-dye separation tests revealed a significant reduction in concentration. All the membranes showed a yield of over 99%, which demonstrates the potential of these membranes for this application.

Keywords: *Membrane, hybrid, polyamide, silicon carbide, dye.*

1. Introduction

One of the main challenges facing society today is the increasing pollution of water. Water pollution occurs when one or more harmful substances are introduced into a water body, negatively impacting its quality[1]. Humanity has known the pigment process for millennia, historical sources date the existence of the textile dyeing industry back more than 4000 years; dyes are organic compounds capable of coloring textile or non-textile substrates and are characterized by absorbing light in the uniform visible UV region[2,3].

The textile wastewater is one of the worst polluters, causing countless problems for living beings. When it comes to human health, ingesting dyes can cause cancer, allergies, dermatitis and mutagenesis, among other health problems. Various techniques have therefore been applied to solve this problem. Some of these techniques are flocculation, biological treatment, advanced oxidation process, adsorption and membrane separation technology[1,4,5].

It is now indisputable that membrane separation processes (MSP) have gained an important place in technology and are used in a wide range of applications due to their numerous benefits. In this context, the industry's great interest in understanding and reducing the costs of such applications has led to a growing number of studies using MSP to treat effluents containing textile dyes[6].

Membranes can be defined as a selective barrier between two phases, which totally or partially restricts the transport of chemical species present, the term selective being inherent to a membrane or a membrane process[7]. The technology involved in MSP uses the mimicking of a natural membrane by means of a synthetic material. Membrane separation involves the separation of chemical species across the membrane interphase by the difference in transport rate[5,7].

The phase inversion technique is the most widely used for producing microporous polymeric membranes; this technique is characterized by the destabilization of a polymeric solution obtained by inducing a state of supersaturation in it, promoted by changes in its chemical nature, composition, temperature or pressure[7]. The most widely used method for obtaining polymeric membranes is immersion-precipitation, which consists of preparing a polymer solution, which is deposited on a molded glass plate to form a thin film. This film is then immersed in a non-solvent bath, usually water. For the polymer, the process can be divided into five steps: (i) preparation of the polymer solution; (ii) deposition of the solution on the glass plate to form the film; (iii) immersion of the film in a precipitation bath; (iv) removal of residual solvent from the polymer matrix formed; and (v) drying of the membrane. Precipitation occurs due to the exchange of solvent for a non-solvent, promoting the destabilization of the polymer solution until the formation of the solid structure of the membrane[7].

Membranes can be classified into two categories: dense or porous; the main properties of a membrane: permeability, selectivity, mechanical resistance, chemical resistance and resistance to fouling depend directly on the materials and methods used to obtain them[8,9]. Synthetic membranes are made from two distinct classes of materials: organic and inorganic[7].

Since the end of World War II, the materials industry has excelled in synthetic polymer technology. Polyamides are a group of these synthetic polymers with excellent mechanical properties[10]. Among engineering polymers, polyamides are

*e-mail: keilamedeiros@ufrb.edu.br
Associate Editor: Leonardo Gondim de Andrade e Silva.
Editor-in-Chief: Luiz Antonio Pessan.

the most widely used due to their excellent balance between cost and performance, and are one of the most widely used polymers for membranes[9,11,12].

Polyamide membranes offer the advantage of being a hydrophilic material, there are several studies reporting on their performance, polyamide membranes are used in applications from microfiltration to reverse osmosis[13-17]. According to Kondo et al.[10], the main characteristics of polyamides are: high strength and rigidity, high fluidity, good ductility at low temperatures, high oxygen barrier, good cost/performance ratio, good chemical resistance, resistance to aging at high temperatures and long periods of time. These intrinsic characteristics of polyamides are essential for application in MSP.

Developments in materials science have led to an association between materials and an in-depth understanding of what we call composites. It is now a consensus among researchers that numerous recent technological achievements only became feasible after the advent of composites. A composite can be defined as a physical mixture between two or more phases, so it is understood that the basic characteristic of composites is to combine at least two distinct phases which are called matrix and reinforcement[18]. The fusion of one or more materials has made it possible to create membranes known as hybrids.

The addition of particles of inorganic compounds to polyamide matrices leads to significant changes in the morphological structure of the membranes. In addition, the use of these additives offers a wide range of applications, from microfiltration to reverse osmosis[10,13-17]. The incorporation of materials such as semiconductors, graphene, molybdenum, zirconium and tungsten oxides, carbon nanotubes, zinc, zinc oxide, aluminum, magnetite and titanium dioxide nanoparticles, as well as silicon carbide, calcium carbonate, alumina, carbon-based materials, activated carbon, clays, among others, in polyamide solutions for the manufacture of hybrid membranes, contributes significantly to improving the efficiency in the treatment of water and effluents. This improvement is due to the intrinsic properties of these additives, such as high specific surface area, high functional efficiency, porous structure and hydrophilicity, desirable characteristics in membrane separation processes[19-38]. The incorporation of silicon carbide (SiC) into polyamide membranes improves their thermal, chemical and mechanical resistance, in addition to increasing hydrophilicity and separation efficiency, making these membranes suitable for operations in severe conditions and for the efficient removal of contaminants such as dyes, oils, heavy metals and suspended particles. SiC can be functionalized to improve its dispersion in the polymer matrix or add functional groups that interact with specific pollutants and is considered safe and non-reactive for use in drinking and industrial water treatment systems.

The automotive industry generates a lot of polyamide synthetic fiber waste when producing fabrics used to reinforce tires. If discarded without treatment, this waste can harm the environment. Some alternatives for recovering these fibers present in tires have been studied, such as reusing them in cardboard packaging as reinforcement, as part of the raw material in asphalt, producing other plastic compounds, and as an additive for lightweight concrete[39,40]. To avoid this problem, these fibers can be reused to obtain hybrid membranes, a sustainable and low-cost material that is ideal for filtration processes. These membranes help remove contaminants from water, allowing it to be reused for cooling industrial processes or disposed of safely, in compliance with environmental legislation. In addition to reducing the environmental impact, this solution brings savings, as it reduces the production costs of the membranes. Therefore, transforming polymeric waste into raw material for filtration is essential to make the industry more sustainable and efficient. The objective of this work is to obtain microporous membranes from residual fibers with the addition of inorganic particles in a polyamide 6.6 (PA66) matrix to be used in the treatment of effluents containing textile dyes.

2. Materials and Methods

For this work, silicon carbide (SiC) was used as the inorganic particle for preparing the hybrid membranes, purchased from Treibacher Schleifmittel Brazil, according to the manufacturer the material is 96.0% pure. The polymeric matrix used was waste polyamide 6.6 synthetic fibers made available by an automobile industry located in Camaçari – BA, Brazil, two solvents were used to solubilize the polyamide and mix the inorganics in the hybrid solutions during the preparation of the membranes, formic acid - FA (85%) which is a monocarboxylic organic acid, its formula is CH_2O_2, with an average molecular mass of 46 $g.mol^{-1}$, manufactured by Vetec Laboratory Products Ltd.; and hydrochloric acid – HA (37%) which is an inorganic acid, its formula is HCl, with an average molar mass of 36.5 $g.mol^{-1}$, manufactured by Neon Laboratory Products Ltd. The salt used as an additive was magnesium chloride $MgCl_2$, with an average molar mass of 95.211 $g.mol^{-1}$, manufactured by Contemporary Chemical Dynamics Ltd.

The PA66 synthetic fibers and the additives used, SiC and $MgCl_2$, dried in an oven at 80 ºC for 24 hours before mixing them in HA and FA to start preparing the solutions. As described in Table 1, the dissolution of PA66 synthetic fibers, $MgCl_2$, and hybrids with 3% by weight of SiC in HA and FA was aided by magnetic stirrers for a period of approximately 2 hours at a temperature (32 ± 2 °C) and relative humidity of 50%. The prepared solutions were spread onto

Table 1. Composition of polyamide membranes and their hybrids.

Membrane	PA66 (g)	SiC (g)	HA (g)	FA (g)	$MgCl_2$ (g)
PA66-HA	10.0	-	40	-	1
PA66-HA|H	9.4	0.6	40	-	1
PA66-FA	10.0	-	-	40	1
PA66-FA|H	9.4	0.6	-	40	1

*PA66-HA = Polyamide 6.6 produced with hydrochloric acid; PA66-FA = Polyamide 6.6 produced with formic acid; **PA66 = Polyamide 6.6; H = Hybrid.**

glass plates using glass rods and then immediately placed in a water bath so that the plates were completely submerged in water at room temperature (31 ± 2 °C). This procedure was carried out in an exhaust hood. The membranes remained in the bath until their precipitation was completely complete. They were then removed from the plates, washed and then submerged in a mixture of 10% hexane and 90% water to prevent the membrane pores from collapsing.

2.1. Characterization of SiC

The silicon carbide was passed through a 200 mesh sieve for particle size distribution on a Mastersizer Malvern Instruments model 2000 laser diffraction particle size analyzer (granulometer). The XRD analysis of the SiC was carried out on a Shimadzu XRD-6000 X-ray diffractometer with copper kα radiation and a scan from 5 to 80º. Subsequently, the SiC was analyzed using HighScore Plus software and the Powder Diffraction File (PDF) of the SiC sample was obtained from the Crystallography Open Database (COD).

2.2. Bubble point (maximum radius of pores)

The bubble point method was used to measure pores over 50 nm in size and is standardized by ASTM International F316-03[41] and from the normal we can obtain the maximum radius of the pores present in the membrane. The method consists of measuring the pressure required to flow a gas (air or N_2) through a membrane whose pores are filled with a liquid. The maximum radius of the pores using the bubble point test can be determined using Equation 1[12].

$$Rp_{máx} = \frac{2\sigma\cos\theta}{P} \quad (1)$$

$Rp_{máx}$ is the radius of the pore, assuming it has a cylindrical shape; σ is the surface tension; θ is the contact angle and ΔP is the pressure difference between the two sides of the membrane.

2.3. Water absorption

The water absorption capacity was measured by placing the membranes with different masses in contact with water. The system kept at a temperature of 24 °C ± 1. The membranes were weighed before and after 24 hours of water absorption. The experiment conducted in triplicate. The percentage of water content was measured by the difference in weight between the dry and wet membranes, expressed using the Equation 2[42].

$$Water\ absorption(\%) = \left[\frac{(W_W - W_d)}{W_w}\right] X\,100 \quad (2)$$

Where W_w and W_d are the masses of the wet and dry membrane, respectively.

2.4. Porosity

Porosity was determined by immersing the membranes in water for 24 hours. This considered the initial mass of the membranes, the absorbed mass of water, the relative volume of the membranes and the density of the penetrating liquid, which is water. The experiment was carried out in triplicate, expressed by Equation 3[12].

$$\varepsilon = \left[\frac{(W_W - W_d)}{V_m \rho_a}\right] \quad (3)$$

Where W_w (g) and W_d (g) are the masses of the wet and dry membrane, respectively. $V_m\left(cm^3\right)$ is the volume of the membrane and $\rho_a\left(g.cm^{-3}\right)$ the density of water in 25 ºC.

2.5. Contact angle

The contact angle (CA) of the membranes analyzed using a Contact Angle Meter, obtained from Alcalitech Manufacture of Apparatus and Measuring Equipment, Model AGC 001. The drop formed manually by means of a micrometric dispenser, and the image of the drop was captured by the camera built into the equipment, where it was analyzed in the software. The contact angle defined as the angle formed between the solid/liquid interface.

2.6. Flow measurements

For the continuous water flow measurement tests, a perpendicular filtration cell coupled to a filtration system was used to measure the permeate. The membranes were subjected to permeability tests at a pressure of 1.0 bar. The effluent flow measurements were carried out in the same perpendicular filtration cell using a concentration of 500 mg.L^{-1}. The textile dye used to produce the synthetic effluent was the commercial Tupy Red 15 dye, from the manufacturer Tupy Dye Industry and Commerce Ltd., Red 15 is a non-toxic azo dye. The performance of the membranes can be assessed through the permeate flux and the selectivity of a particular solute present in the feed solution. The flow (J) for the membranes with pure PA with different acids and PA with 3% SiC was determined using Equation 4.

$$J = \frac{Permeate\ volume(L)}{Time(h)\ x\ Membrane\ area\left(m^2\right)} \quad (4)$$

2.7. Average pore radius

The equation used to find the Average Pore Radius is the Guerout-Efford-Ferry Equation[42], where η is the viscosity of water (8.9 × 10^{-4} Pa.s); l is the average thickness of each membrane (m), which was measured using an Asimetro Outside MIC micrometer; Q is the permeate flow (m^3.s^{-1}); ε is the porosity (admensional) determined by Equation 4; P is the transmembrane operating pressure (Pa) and A is the membrane area (m^2), as shown in Equation 5:

$$\text{Average Pore Radius} = \sqrt{\frac{8\eta l Q(2.9 - 1.75\varepsilon)}{\varepsilon P A}} \quad (5)$$

2.8. Membrane backwash

Each backwashing experiment consisted of distinct stages which included: initial flow of pure water, rinsing with water to remove residual material and then the final flow with pure water. The membranes were subjected to permeability tests at a pressure of 1.0 bar with dye, the permeate was collected

at an interval of 3 min, for a total period of 30 min for each membrane, totaling 10 collections. The backwashing time and pressure chosen were based on the literature: 1 minute with a pressure of 1.5 bar[43]. The membranes were then subjected to permeability tests again at a pressure of 1.0 bar with the dye. The volume of water used calculated according to Equation 6:

$$Water\,used = \frac{V_R}{V_T} \quad (6)$$

The V_R e V_T are the masses of water from backwashing and total flow over 30 min, respectively.

Backwashing efficiency measured according to Equation 7:

$$\eta a = \frac{Lp}{Lp_0}\ X100\% \quad (7)$$

Lp is the flow after backwashing divided by the permeation pressure, and Lp_0 is the backwashing flow divided by the backwashing pressure.

2.9. Textile dye concentration

The absorbance analyses of the effluent containing textile dye after permeation and backwashing tests were conducted using a UV-vis Kasuaki spectrophotometer, model IL - 593 - BI.

2.10. Membrane efficiency

The membranes efficiency was estimated by the rejection coefficient (R%) or yield, calculated based on the ratio of the dye concentrations in the permeate (C_p) and in the feed (C_0) expressed using Equation 8[13].

$$R(\%) = \left[\frac{(C_o - C_p)}{C_o}\right] X100\% \quad (8)$$

3. Results and Discussion

3.1. Particle size distribution and X-ray diffraction

Figure 1 shows the particle size distribution, which was of the bimodal type with a wide distribution range and an average particle diameter of around 1.38 µm. The distribution range extends from 0.04 µm to approximately 5 µm. And around 60.6% of the accumulated particles are smaller than 2 µm. In addition, 10% of the particles have diameters smaller than 0.09 µm, 50% of the particles have diameters smaller than 0.38 µm and 90% of the particles have diameters smaller than 3.18 µm.

The X-ray diffraction of the SiC sample is shown in Figure 2. The material has considerable crystallinity and is mostly composed of a single phase. The phase of the SiC crystals can be identified by the diffraction planes (101), (103) around the most intense diffraction peak (102)[44]. All the reflections observed can be indexed in symmetry, with interplanar spacings reported in the literature for polytype: SiC-6H (PDF – 96-901-0159)[45,46].

3.2. Contact angle

Figure 3 shows how the polyamide 6.6 membranes behaved with the use of different solvents and the addition of SiC. The pure membranes had higher contact angle (CA) values when compared to their hybrid counterparts. The PA66-FA membrane recorded the highest contact angle, probably due to the low roughness of its surface layer. At the initial time of 5 seconds, its contact angle was 84.55°, with a slight decrease over time, reaching 77.32° at the final time of 45 seconds. In the case of the PA66-HA membrane, the initial contact angle was 56.90° at 5 seconds, with a

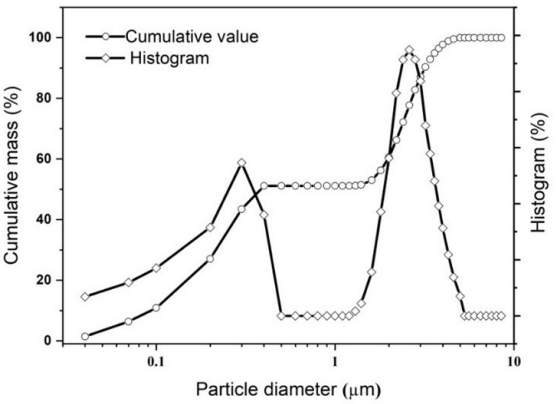

Figure 1. Particle size distribution of silicon carbide.

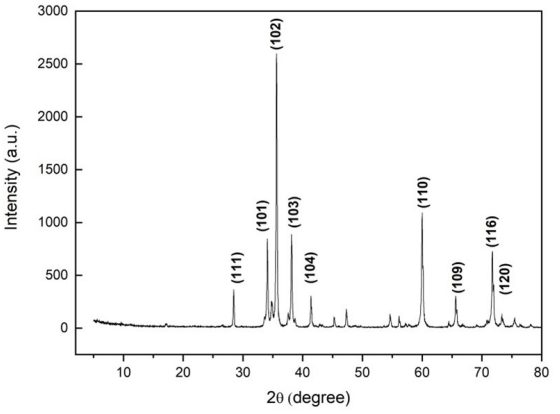

Figure 2. X-ray diffraction of SiC.

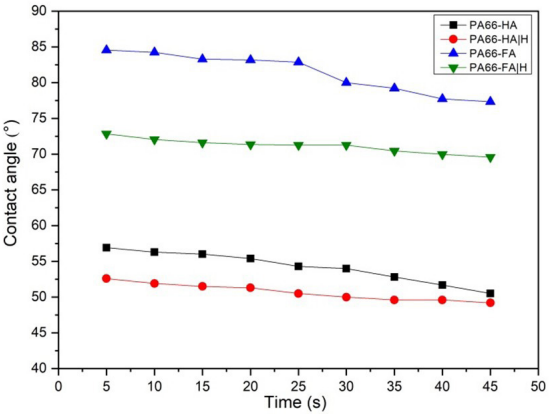

Figure 3. Membranes contact angle.

slight reduction, reaching 50.50° after 45 seconds. The microfiltration membranes prepared showed high contact angles, consistent with studies in the field[16,46,47].

At the initial test time of 5 s, the PA66-FA|H and PA66-HA|H membranes showed values of 72.83° and 52.60° respectively, and at the end of the test the values found were 69.59° and 49.20°. The addition of 3% by weight of SiC to the polymer solutions gave lower contact angle values compared to the pure membranes, regardless of the acid used, possibly due to the formation of a morphological structure with a rougher surface on the hybrid membranes. The hydrophilic properties of the surface of the polyamide 6.6 material allow all the membranes to have a large contact angle, but the addition of SiC led to a decrease in these values. Improvements in permeability are directly associated with CA, the smaller the contact angle the greater the permeate flux; the membrane with the highest hydrophilicity was PA66-HA|H. The incorporation of SiC in membranes with a polyamide matrix, regardless of the solvent used in the preparation of the hybrid membranes, increased hydrophilicity and, consequently, will positively influence the separation efficiency.

3.3. Water absorption and porosity

Figure 4 shows the percentage of water absorbed in 24 hours, with the PA66-HA membrane showing water absorption of (73.71 ± 0.45) %; the PA66-HA|H membrane showed (76.08 ± 0.92) % water absorption; the PA66-FA membrane showed (24.84 ± 6.59) % and the PA66-FA|H membrane showed (23.53 ± 2.68) % water absorption. For the samples obtained with hydrochloric acid, the hybrid membranes showed higher water absorption compared to the pure membrane, which may indicate a porogenic action of the SiC. However, this was not the case for the membranes obtained with formic acid, where the SiC seems to have had no effect or showed a densifying effect (generating agglomerates); it can be seen that the pure membrane obtained with formic acid showed a water absorption value similar to that of the hybrid membrane. It is important to emphasize that SiC has an inherently hydrophilic surface, promoting greater affinity with water and a lower tendency to form fouling (incrustation). It has a porous structure and high surface area, which can contribute to the modification of the membrane morphology, increasing the active separation area and improving the adsorption and size exclusion mechanisms, favoring the increase in permeate flux and the efficiency of the filtration process.

Figure 5 shows the porosities obtained. The membranes obtained with hydrochloric acid had higher PA66-HA porosity values with water absorption of (66.67 ± 0.85) %, while the PA66-HA|H hybrid membrane had (73.86 ± 1.89) %. The membranes obtained with formic acid showed low porosity, the PA66-FA membrane showed (37.19 ± 6.70) % and the PA66-FA|H hybrid membrane showed (36.70 ± 6.88) %.

The lower value for water absorption and, consequently, porosity may be a result of the morphology of the membrane prepared with formic acid, in which the thickness of the membrane is relatively high (~350μm). The dissolution stage of the membrane is of paramount importance in the formation of the film and its performance. Poletto et al.[48] obtained polyamide 6.6 membranes, also using formic acid and hydrochloric acid, and the authors reported that the membrane prepared with hydrochloric acid had lower porosity compared to the one prepared with formic acid. In principle, the reason for this difference can be attributed to the solvent evaporation time, in the work, authors speculate that the high solvent evaporation time led to low porosity for the formic acid membranes[17,48].

Another important point was the addition of SiC, which behaved differently when in contact with the different acids. When used with HCl, the desired effect was an increase in porosity[14,49]. However, in contact with FA, SiC had a densifying effect. Yan et al.[16] in an attempt to produce a UF membrane, graphene oxide (GO) was incorporated into a polyamide 6.6 matrix, the values tested were 0%, 0.1%, 0.3% and 0.5% by weight, and what was observed was that the porosity of the ultrafiltration membrane decreased as graphene oxide was added, The authors pointed out that with the addition of GO, the viscosity of the solution gradually increased, hindering the phase separation process and resulting in a final membrane with a relatively dense structure.

3.4. Maximum pore radius and average pore radius

Figure 6 shows the maximum pore radius of the membranes obtained. Figure 6 shows that the PA66-HA; PA66-HA|H; PA66-FA; PA66-FA|H membranes had maximum pore radii of

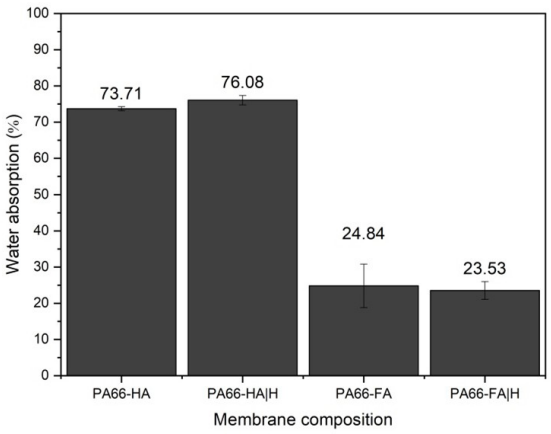

Figure 4. Membrane water absorption.

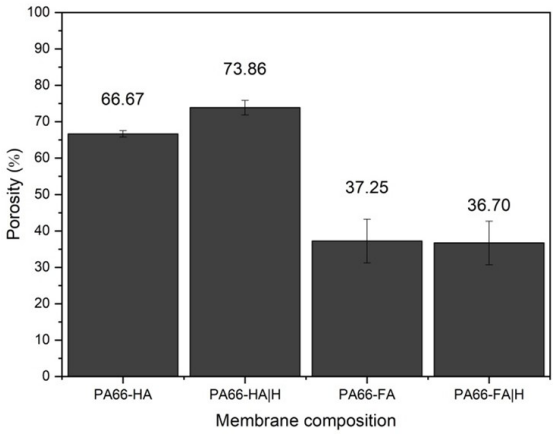

Figure 5. Membrane porosity.

approximately 1.68; 1.78; 6.82 and 3.01 µm, respectively. The membrane with the smallest pore radius was PA66-HA, with an increase in pore radius for the PA66-HA|H hybrid; however, the opposite happened for the membranes solubilized in formic acid, further strengthening the idea that SiC acted as a densifier, as the PA66-FA membrane had a pore size approximately 2.3 times larger than the PA66-FA|H membrane. Chang et al.[50] when calculating the bubble point for polyamide 6.6 membranes, showed that the concentration of the materials used will influence the maximum pore size, what the authors reported is that the pore size grew according to the solvent concentration.

Figure 7 shows the average pore radius of the membranes produced. Using the Guerout-Elford-Ferry formula, it was possible to find the average pore radius. The PA66-HA membrane has an average pore size of (0.132 ± 0.002) µm, the second composition with the addition of SiC particles, the PA66-HA|H membrane, has an average pore size of (0.159 ± 0.003) µm. The PA66-FA membrane has (0.230 ± 0.028) µm, while its hybrid pair the PA66-FA|H membrane has (0.148 ± 0.018) µm.

The larger pore radius present in the PA66-FA membrane found in the bubble point and average pore radius results can be attributed to the interaction of magnesium chloride with formic acid. Medeiros et al.[11] observed that the use of inorganic salts causes phenomena that can contribute to an increase in pores. They reported that the addition of calcium chloride ($CaCl_2$) to pure polyamide 6 membranes and hybrid membranes caused an increase in the size and distribution of pores.

All the membranes demonstrated are within the range that would be characteristic for microfiltration MSP and are compatible with other studies in the literature[12,50]. Here we can highlight the dual effect of SiC, which depends on the solvent. Its porogenic action was observed when combined with HCl and a densifying action when combined with FA.

3.5. Water and effluent flow measurements

The water mass flux measurement tests (J_0) were carried out using a pressure of 1.0 bar. Figure 8 shows the curves of the flux measurements made with distilled water of the PA66-HA, PA66-HA|H, PA66-FA and PA66-FA|H membranes.

The measurements of the flux permeated with water for the membranes produced with HCl initially showed a decrease, followed by stability at approximately 30 min. The PA66-HA membrane did not show great variations, with a very low flux. These results are in line with those previously reported by the average pore size radius, confirming the presence of very small pores. The PA66-HA|H membrane had the highest flux, but showed a considerable drop in flux, due to a mechanical compaction phenomenon caused by the pressure applied and/or possible swelling in the membranes, since when the membrane comes into contact with water, it causes a gradual reduction in the pores, thus reducing its permeability[46]. Due to this phenomenon, additive is preferred, and compared to its pure counterpart, the hybrid membranes proved to be far superior. Furthermore, SiC has high hardness and mechanical strength, increasing the structural robustness of the membrane, which can reduce possible deformations and mechanical wear of the hybrid membranes during operation.

When analyzing the membranes obtained with FA, both had a low flux compared to the membranes obtained with HCl. This difference can be attributed to the fact that these membranes have lower porosity and denser thicknesses; the HCl membranes were obtained with a thickness of ~250 µm, while the FA membranes were obtained with ~350 µm. The PA66-FA membrane showed a higher flux than the PA66-FA|H hybrid membrane, which was the opposite of the membranes

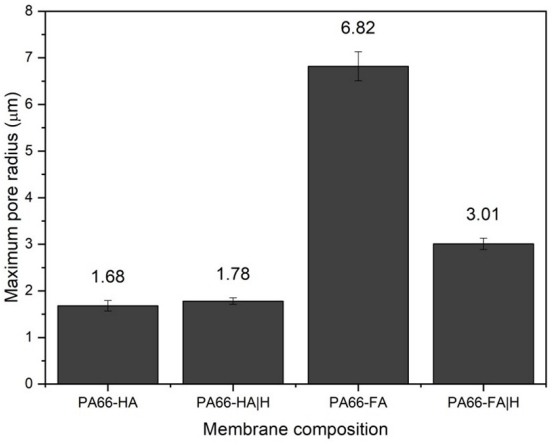

Figure 6. Maximum membrane pore radius.

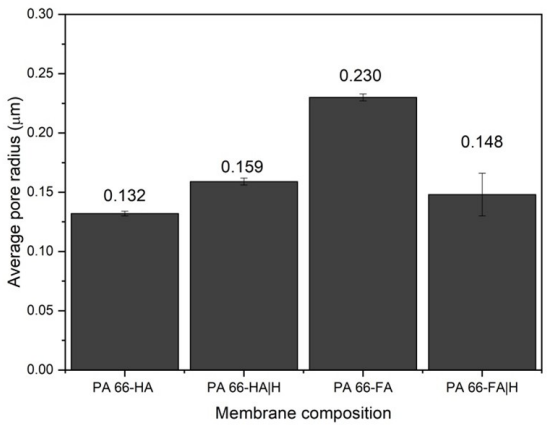

Figure 7. Average membrane pore radius.

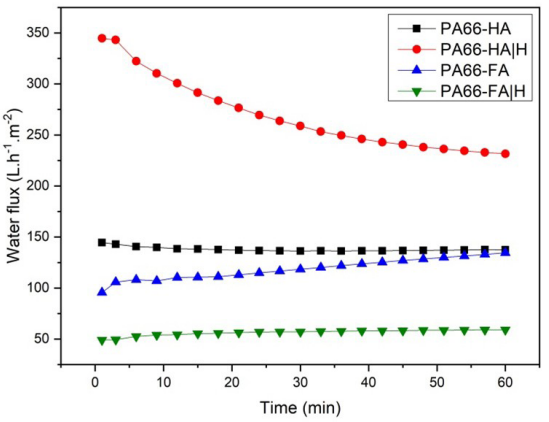

Figure 8. Permeate flux of water at a pressure of 1 bar.

obtained with HCl. This was due to the densification caused by the SiC, which clogged some of the membrane's pores.

Unlike the membranes obtained with HCl, those obtained with FA did not show the phenomenon of mechanical compaction; on the contrary, in a certain range there was an increase in flux (Table 2). This phenomenon can be attributed to the momentary relaxation of the pores due to the temperature; the measured temperature of the liquid present in the tubes of the equipment responsible for the flux reached a temperature of 50 ± 2 ºC. SiC is an advanced ceramic material with exceptional properties, which makes it an excellent choice to be incorporated into polyamide membranes in order to improve their performance in separation applications, especially in aggressive environments, such as water and industrial effluent treatment. SiC has excellent thermal resistance, withstands high temperatures without degradation, allowing its use in thermal processes or with temperature variations. A similar behavior was observed by Poletto et al.[48] when performing a flux on a polyamide 6.6 membrane and noticing a gradual increase in flux over a certain period of time.

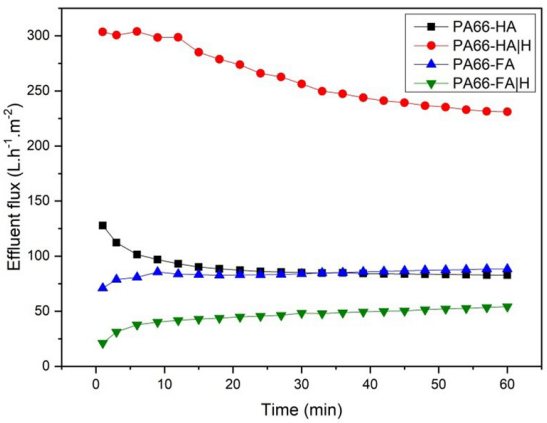

Figure 9. Permeate effluent flux at a pressure of 1 bar.

The pollutant mass flow measurement tests (J) were carried out using a pressure of 1.0 bar. Figure 9 shows the curves of the flux measurements made with the dye for the PA66-HA, PA66-HA|H, PA66-FA and PA66-FA|H membranes.

In accordance with the pattern found in the water flow tests, Figures 9 shows the same behaviour with the effects found for the water flow, such as concentration polarization, compaction, swelling, pore reduction and, in addition to the use of a pollutant, the fouling effect, i.e. the filling of the pores by the particulate material present in the effluent[51]. Figure 10 shows the intensity of the color of the material retained on the surface of the membrane, the fouling that occurred with the gradual filling of the membrane pores by the dye particles. This can be seen in Table 3 when we compare the effluent flow values with the pure water values in Table 2.

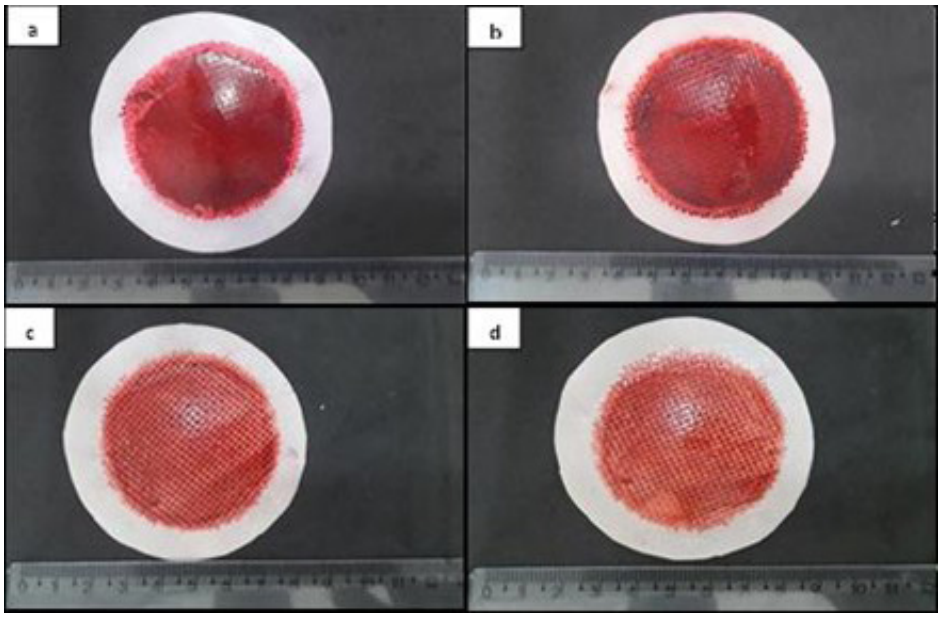

Figure 10. Surface of PA66 membranes after flux with effluent a) PA66-HA, b) PA66-HA|H, c) PA66-FA, d) PA66-FA|H.

Table 2. Initial, intermediate and final water flux values obtained by the membranes for pressure of 1 bar.

Composition	Initial Flux ($L.m^{-2}.h^{-1}$) 1 min	Intermediate Flux ($L.m^{-2}.h^{-1}$) 30 min	Final Flux ($L.m^{-2}.h^{-1}$) 60 min
PA66-HA	144.65	136.27	137.56
PA66-HA|H	344.73	258.78	231.60
PA66-FA	95.71	118.50	134.51
PA66-FA|H	48.93	57.18	59.10

The mass flow measurements when separating the dye in water (J) from the membranes were plotted in reference to the mass flow of water (J_0), i.e. J/J_0. The influence of the dye concentration on the flux factor (J/J_0) of the membranes can be seen in Figure 11.

The pure membranes, regardless of the acid used to obtain them: PA66-HA and PA66-HA, showed a decrease over 30 minutes and then stability in these ratios, probably due to compaction or swelling in the membranes, as seen in the water flow measurements. Another factor responsible for the relative decline in the permeability of the unmodified membranes was influenced by the adsorption of dye molecules on the surface[51].

A certain amount of molecules is adsorbed on the surface of the pores, and this can result in the formation of a film on the inner surface of the membrane, a similar phenomenon was observed by Arahman et al.[52] in polyethersulfone (PES) membranes, it was observed that membranes with high hydrophilicity can reduce the adsorption of molecules on the surface of the membrane pores, as a consequence, the formation of the fouling layer can be minimized and therefore the relative permeability of this membrane does not change significantly. The hybrid membranes showed a progressive increase and maintained a higher J/J_0 ratio over time compared to the pure membranes at the same pressures. We can assume that because of the added SiC load, there was an increase in the hydrophilicity of the membranes according to the contact angle results shown in Figure 3.

Membrane fouling is a common phenomenon in microfiltration membrane separation processes that significantly impair filtration efficiency. This makes membrane regeneration an integral part of microfiltration systems and necessitates the need for effective membrane cleaning in order to maintain greater efficiency of the separation process[53].

3.6. Membrane backwash

The chemical resistance of the membrane is essential to withstand multiple backwash cycles (backwashing or chemical cleaning), especially in water and effluent treatment applications. Backwashing often involves acidic, alkaline or oxidizing solutions (e.g. hypochlorite, citric acid, sodium hydroxide) which are aggressive chemical agents to remove organic, inorganic or biological fouling. A membrane with low chemical resistance degrades or loses performance after repeated exposures. Chemical degradation can alter the morphology of the membrane (porosity, surface charge), compromising the rejection of contaminants. Chemical resistance ensures selectivity stability over time. Therefore, materials with high chemical resistance, such as SiC-modified membranes, maintain their structural and functional properties even after multiple cleanings, reducing replacement frequency and operating cost.

Figure 12 illustrates the effect of the backwashing conducted to evaluate the reduction in membrane fouling and the improvement in membrane cleaning efficiency. The procedure led to an increase in flux for all the membranes. The PA66-HA|H membrane showed the greatest initial growth with probable dilation of its pores, but over the course of 30 min, there was a drop in flux associated with the formation of fouling; while the PA66-HA membrane followed its observed flux pattern, backwashing not generating large increases in flux. However, the pure and hybrid membranes

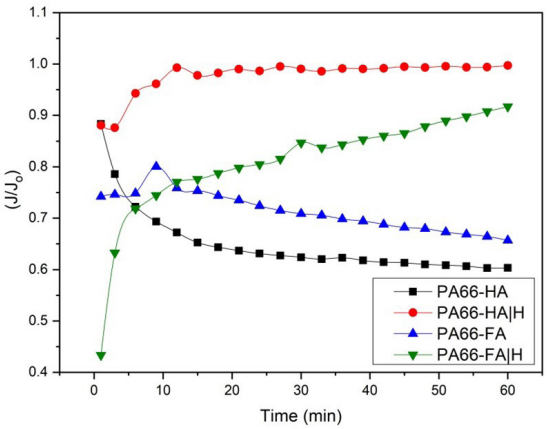

Figure 11. Influence of the dye concentration on the flux factor (J/J_0) of the membranes.

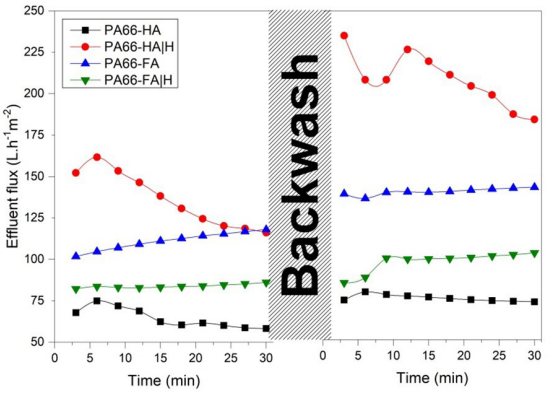

Figure 12. Influence of backwashing on membrane flux at a concentration of 500 $mg.L^{-1}$ and a pressure of 1.0 bar; the left side represents the moment before backwashing and the right side after the backwashing process.

Table 3. Initial, intermediate and final effluent flux values obtained by the membranes at a pressure of 1.0 bar.

Composition	Initial Flux ($L.m^{-2}.h^{-1}$) 1 min	Intermediate Flux ($L.m^{-2}.h^{-1}$) 30 min	Final Flux ($L.m^{-2}.h^{-1}$) 60 min
PA66-HA	127.76	85.01	83.00
PA66-HA|H	303.59	256.27	230.96
PA66-FA	71.02	83.99	88.35
PA66-FA|H	21.22	48.41	54.20

made with formic acid show progressive increase in their continuous flux was slightly modulated by backwashing.

Table 4 shows the values for the volume of water used and the backwashing efficiency. We can see that there appears to be a relationship between the volume of water used and efficiency. The PA66-FA membrane had the lowest volume and the highest efficiency, which we can relate to the progressive increase in its flow over time. However, PA66-FA showed the worst performance with an efficiency value of 14.53%.

Membranes with high chemical resistance, such as those modified with silicon carbide, are more durable, stable and efficient in systems that require frequent backwashing, ensuring better performance over time and lower maintenance costs, as SiC has high chemical resistance due to a stable material in acidic and alkaline environments, resists oxidizing agents and organic solvents and is ideal for applications in aggressive environments, such as industrial effluents contaminated with dyes.

3.7. Dye concentration and membrane efficiency

Through spectrophotometric analysis, it was possible to identify the peak wavelength of the dye, from which an absorbance curve was plotted. These curves are shown in Figure 13, where the peak wavelength is highlighted at 505 nm. This value indicates the wavelength at which the dye shows maximum light absorption.

From the 505 nm wavelength value, the absorbance calibration curve of the red dye was plotted at all concentrations (0 $mg.L^{-1}$ to 500 $mg.L^{-1}$), resulting in Figure 14, where it was possible to obtain the straight line equation ($y = 0.00129x - 0.00216$) with R^2 0.9977. This indicates that the absorbance results of the dye at each concentration follow a well-fitting function and are therefore useful for correlating with the absorption data of each effluent sample used in the treatment with the membranes produced. From the straight-line equation, it was possible to determine the concentration of dye remaining in the permeate after treatment:

$$\text{Dye concentration} = \frac{y - 0.00216}{0.00129} \quad (9)$$

With the concentration of the dye remaining in the permeates, the efficiency of the polyamide 6.6 membranes in retaining the particulates was found in each case using Equation 9, both parameters are shown in Table 5, with all membranes achieving yields of over 99%. Similar results were found by Liu et al.[31], who prepared polyamide membranes with additives using the phase inversion technique through the immersion precipitation method. Adjustments to the microstructure of the membranes were made with seven commercial ionic surfactants and one self-synthesized surfactant, S20, to improve performance and mechanical strength. As a result, the tensile strength of the membranes and their porosity were improved, since, for example, S20 decreased the molecular weight and consequently the average pore size of the membrane. The membrane that had 50% S20 by weight of the copolymer removed 98% of Congo red dye and 80% of Chrome blue dye, showing promising results in the treatment of textile effluents.

Table 6 shows the performance of the membranes before and after backwashing. It is known that backwashing causes damage to membrane pores and decreases their selectivity, but an insignificant decrease was obtained, thus demonstrating that the time and pressure chosen were adequate[43,50].

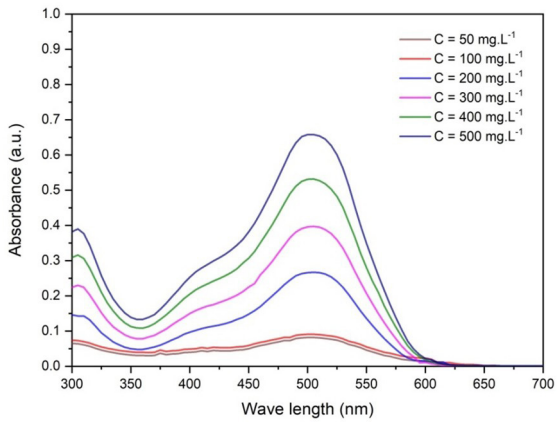

Figure 13. Absorption Specter of the red dye at concentrations of 50 $mg.L^{-1}$, 100 $mg.L^{-1}$, 200 $mg.L^{-1}$, 300 $mg.L^{-1}$, 400 $mg.L^{-1}$ e 500 $mg.L^{-1}$.

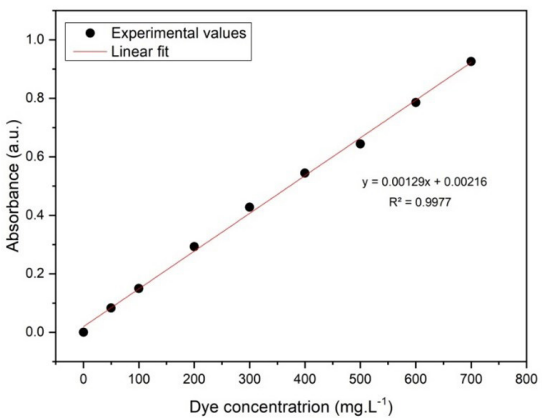

Figure 14. Calibration curve of dye absorbance.

Table 4. Volume of water used and efficiency of membrane backwashing.

Composition	Supply pressure (bar)	Backwash pressure (bar)	Water used	ηa - Backwashing efficiency (%)
PA66-HA	1.0	1.5	0.34	14.53
PA66-HA|H	1.0	1.5	0.17	35.44
PA66-FA	1.0	1.5	0.07	68.35
PA66-FA|H	1.0	1.5	0.11	36.96

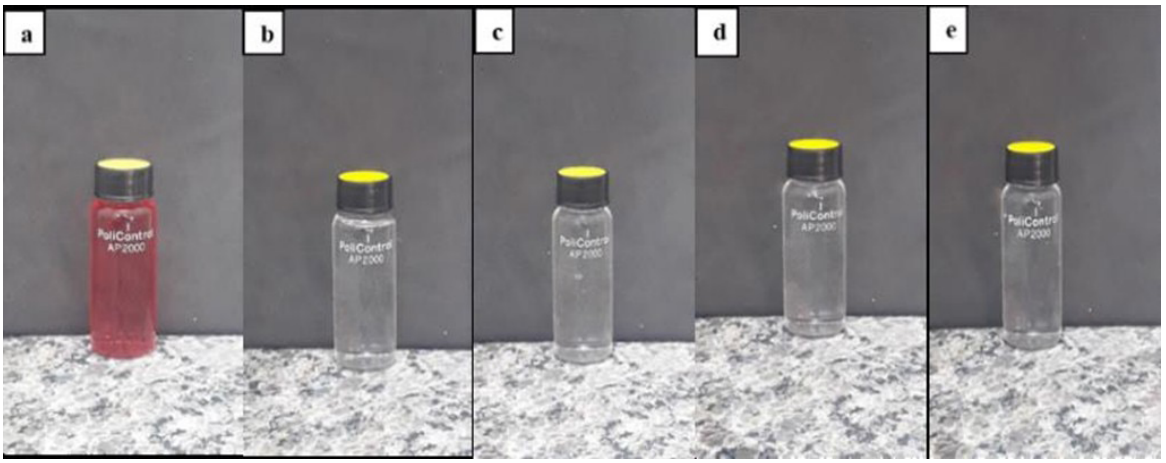

Figure 15. Visual comparison of permeate after flow with effluent a) Concentrate 500 mg.L^{-1} b) PA66-HA, c) PA66-HA|H, d) PA66-FA, e) PA66-FA|H.

Table 5. Concentration of the dye in permeate after 60 min in the dye flow test, for pressure of 1 bar.

Composition	Concentration (mg.L^{-1})	Efficiency (%)
PA66-HA	0.58	99.88
PA66-HA|H	0.93	99.81
PA66-FA	0.88	99.82
PA66-FA|H	1.03	99.79

Table 6. Concentration of the dye in permeate after 30 min in the flow test with dye and backwashing, for pressure of 1.0 bar.

Backwashing	Composition	Concentration (mg.L^{-1})	Efficiency (%)
Before	PA66-HA	0.52	99.89
	PA66-HA|H	1.09	99.78
	PA66-FA	0.58	99.88
	PA66-FA|H	0.52	99.89
After	PA66-HA	0.58	99.88
	PA66-HA|H	1.44	99.71
	PA66-FA	1.03	99.79
	PA66-FA|H	0.63	99.87

Figure 15 shows the visual aspects of the permeates, with a sudden change in color from the raw effluent to the permeate obtained, proving the efficiency in separating the dye by the membranes and the potential of these membranes to be applied in the treatment of textile effluents.

4. Conclusion

It was possible to successfully obtain pure and hybrid PA66 membranes with different solvents from PA66 yarn waste from the automotive industry. The membranes obtained with formic acid showed low water absorption and low porosity compared to the membranes obtained with hydrochloric acid. The pure formic acid membranes had larger pore sizes due to the interaction with the inorganic salt, while those obtained with hydrochloric acid had the smallest pore sizes. It observed that silicon carbide can perform distinct functions depending on the acid used. The contact angle values showed that there was an increase in the hydrophilicity of the hybrid membranes containing 3% SiC. Backwashing proved to be efficient, restarting flows without damaging the membrane's permeability and selectivity. The results obtained show that these are microfiltration-scale membranes that have the potential to use in the treatment of wastewater containing textile dyes. The membranes produced from the reuse of polyamide showed more than 99% efficiency in removing the textile dye used.

5. Acknowledgements

The authors would like to thank the Brazilian National Council for Scientific and Technological Development (CNPq), the Coordination for the Improvement of Higher Education Personnel (CAPES), the Bahia State Research Support Foundation (FAPESB) and he grant #2393/2023-d, Paraiba State Research Support Foundation (FAPESQ) for their financial support.

6. References

1. Crini G, Lichtfouse E. Advantages and disadvantages of techniques used for wastewater treatment. Environ Chem Lett. 2019;17(1):145-55. http://doi.org/10.1007/s10311-018-0785-9.
2. Benkhaya S, M′ rabet S, El Harfi A. A review on classifications, recent synthesis and applications of textile dyes. Inorg Chem Commun. 2020;115:107891. http://doi.org/10.1016/j.inoche.2020.107891.
3. Bianchini R, Cevasco G, Chiappe C, Pomelli CS, Rodríguez Douton MJ. Ionic liquids can significantly improve textile dyeing: an innovative application assuring economic and environmental benefits. ACS Sustain Chem& Eng. 2015;3(9):2303-8. http://doi.org/10.1021/acssuschemeng.5b00578.
4. Bera SP, Godhaniya M, Kothari C. Emerging and advanced membrane technology for wastewater treatment: a review. J Basic Microbiol. 2022;62(3-4):245-59. http://doi.org/10.1002/jobm.202100259.
5. Oyarce E, Roa K, Boulett A, Sotelo S, Cantero-López P, Sánchez J, et al. Removal of dyes by polymer-enhanced ultrafiltration: an

overview. Polymers. 2021;13(19):3450. http://doi.org/10.3390/polym13193450.
6. Al-Tohamy R, Ali SS, Li F, Okasha KM, Mahmoud YAG, Elsamahy T, et al. A critical review on the treatment of dye-containing wastewater: ecotoxicological and health concerns of textile dyes and possible remediation approaches for environmental safety. Ecotoxicol Environ Saf. 2022;231:113160. http://doi.org/10.1016/j.ecoenv.2021.113160.
7. Mulder M, Mulder J. Basic principles of membrane technology [Internet]. Dordrecht: Springer Netherlands; 1996 [cited 2025 Jan 9]. Available from: https://books.google.com.br/books?id=SP2%5C_GYvL384C
8. Warsinger DM, Chakraborty S, Tow EW, Plumlee MH, Bellona C, Loutatidou S, et al. A review of polymeric membranes and processes for potable water reuse. Prog Polym Sci. 2018;81:209-37. http://doi.org/10.1016/j.progpolymsci.2018.01.004.
9. Tibi F, Charfi A, Cho J, Kim J. Fabrication of polymeric membranes for membrane distillation process and application for wastewater treatment: critical review. Process Saf Environ Prot. 2020;141:190-201. http://doi.org/10.1016/j.psep.2020.05.026.
10. Kondo MY, Montagna LS, Morgado GFM, Castilho ALG, Batista LAPS, Botelho EC, et al. Recent advances in the use of Polyamide-based materials for the automotive industry. Polímeros. 2022;32(2):e2022023. http://doi.org/10.1590/0104-1428.20220042.
11. Medeiros KM, Araújo EM, Lira HL, Lima DF, Lima CAP. Hybrid membranes of polyamide applied in treatment of waste water. Mater Res. 2017;20(2):308-16. http://doi.org/10.1590/1980-5373-mr-2016-0242.
12. Ebrahimi M, Kujawski W, Fatyeyeva K. Fabrication of polyamide-6 membranes: the effect of gelation time towards their morphological, physical, and transport properties. Membranes. 2022;12(3):315. http://doi.org/10.3390/membranes12030315.
13. Medeiros KM, Medeiros VN, Lima DF, Lima CAP, Araújo EM, Lira HL. Hybrid microporous membranes applied in wastewater treatment. Macromol Symp. 2019;383(1):1800037. http://doi.org/10.1002/masy.201800037.
14. Huang L, Bui NN, Meyering MT, Hamlin TJ, McCutcheon JR. Novel hydrophilic nylon 6,6 microfiltration membrane supported thin film composite membranes for engineered osmosis. J Membr Sci. 2013;437:141-9. http://doi.org/10.1016/j.memsci.2013.01.046.
15. Mo JH, Lee YH, Kim J, Jeong JY, Jegal J. Treatment of dye aqueous solutions using nanofiltration polyamide composite membranes for the dye wastewater reuse. Dyes Pigm. 2008;76(2):429-34. http://doi.org/10.1016/j.dyepig.2006.09.007.
16. Yan J, Nie L, Li G, Zhu Y, Gao M, Wu R, et al. Graphene oxide modified polyamide 66 ultrafiltration membranes with enhanced anti-fouling performance. Membranes. 2022;12(5):458. http://doi.org/10.3390/membranes12050458.
17. Zeni M, Riveros R, Souza JF, Mello K, Meireles C, Rodrigues GR Fo. Morphologic analysis of porous polyamide 6,6 membranes prepared by phase inversion. Desalination. 2008;221(1-3):294-7. http://doi.org/10.1016/j.desal.2007.03.012.
18. Sachdeva A, Singh PK, Rhee HW. Composite materials: properties, characterization, and applications. London: Taylor & Francis Group LLC; 2021 [cited 2025 Jan 9]. Available from: https://books.google.com.br/books?hl=pt-BR&lr=&id=Dc0QEAAAQBAJ&oi=fnd&pg =PP1&dq=Composite+materials:+properties,+characterization,+and+applications&ots =2cN3mI6cUK&sig=KPbUGVT60BYsE6sah5KeqnzNLy4&redir_esc=y#v=onepage& q=Composite%20materials%3A%20prop
19. Zhi SH, Wan LS, Xu ZK. Poly(vinylidene fluoride)/poly(acrylic acid)/calcium carbonate composite membranes via mineralization. J Membr Sci. 2014;454:144-54. http://doi.org/10.1016/j.memsci.2013.12.011.
20. Hussain A, Al-Yaari M. Development of polymeric membranes for oil/water separation. Membranes. 2021;11(1):42. http://doi.org/10.3390/membranes11010042.
21. Kacprzyńska-Gołacka J, Łożyńska M, Barszcz W, Sowa S, Wieciński P. Microfiltration membranes modified with zinc by plasma treatment. Membranes. 2023;13(4):387. http://doi.org/10.3390/membranes13040387.
22. Aghili F, Ghoreyshi AA, Van der Bruggen BVD, Rahimpour A. Introducing gel-based UiO-66-NH2 into polyamide matrix for preparation of new super hydrophilic membrane with superior performance in dyeing. Wastewater Treat. 2021;9(4):105484. http://doi.org/10.1016/j.jece.2021.105484.
23. Mutharasi Y, Kaleekkal NJ, Arumugham T, Banat F, Kapavarapu MSRS. Antifouling and photocatalytic properties of 2-D Zn/Al layered double hydroxide tailored low-pressure membranes. Chem Eng Process. 2020;158:108191. http://doi.org/10.1016/j.cep.2020.108191.
24. Wang F, Zheng T, Xiong R, Wang P, Ma J. Strong improvement of reverse osmosis polyamide membrane performance by addition of ZIF-8 nanoparticles: effect of particle size and dispersion in selective layer. Chemosphere. 2019;233:524-31. http://doi.org/10.1016/j.chemosphere.2019.06.008.
25. Aziz M, Kasongo G. Scaling prevention of thin film composite polyamide Reverse Osmosis membranes by Zn ions. Desalination. 2019;464:76-83. http://doi.org/10.1016/j.desal.2019.04.021.
26. Xu Z, Li P, Li N, Wang W, Guo C, Shan M, et al. Constructing dense and hydrophilic forward osmosis membrane by cross-linking reaction of graphene quantum dots with monomers for enhanced selectivity and stability. J Colloid Interface Sci. 2021;589:486-99. http://doi.org/10.1016/j.jcis.2021.01.004.
27. Al-Gamal AQ, Falath WS, Saleh TA. Enhanced efficiency of polyamide membranes by incorporating TiO2-Graphene oxide for water purification. J Mol Liq. 2021;323:114922. http://doi.org/10.1016/j.molliq.2020.114922.
28. Urper-Bayram GM, Bossa N, Warsinger DM, Koyuncu I, Wiesner M. Comparative impact of SiO2 and TiO2 nanofillers on the performance of thin-film nanocomposite membranes. J Appl Polym Sci. 2020;137(44):49382. http://doi.org/10.1002/app.49382.
29. Shao F, Xu C, Ji W, Dong H, Sun Q, Yu L, et al. Layer-by-layer self-assembly TiO2 and graphene oxide on polyamide reverse osmosis membranes with improved membrane durability. Desalination. 2017;423:21-9. http://doi.org/10.1016/j.desal.2017.09.007.
30. Tayefeh A, Mousavi SA, Wiesner M, Poursalehi R. Synthesis and surface characterization of magnetite-titania nanoparticles/polyamide nanocomposite smart RO membrane. Procedia Mater Sci. 2015;11:342-6. http://doi.org/10.1016/j.mspro.2015.11.114.
31. Liu D, Zhu Z, Zhao Y, Chen Y, Tan Y, Zhang Y. Low pressure modified polyamide 6 membrane for effective fractionation of dyes and NaCl. Sci Total Environ. 2019;695:133908. http://doi.org/10.1016/j.scitotenv.2019.133908.
32. David PS, Karunanithi A, Fathima NN. Improved filtration for dye removal using keratin–polyamide blend nanofibrous membranes. Environ Sci Pollut Res Int. 2020;27(36):45629-38. http://doi.org/10.1007/s11356-020-10491-y.
33. Isawi H. Development of thin-film composite membranes via radical grafting with methacrylic acid/ZnO doped TiO2 nanocomposites. React Funct Polym. 2018;131:400-13. http://doi.org/10.1016/j.reactfunctpolym.2018.08.018.
34. Santos BPS, Arias JJR, Jorge FE, Santos REPD, Fernandes BS, Candido LS, et al. Preparation, characterization and permeability evaluation of poly (vinylidene fluoride) composites with ZnO particles for flexible pipelines. Polym Test. 2021;94:107064. http://doi.org/10.1016/j.polymertesting.2021.107064.
35. Santos EA Fo, Medeiros KM, Araújo EM, Ferreira RSB, Oliveira SSB, Medeiros VN. Membranes of polyamide 6/clay/salt for water/oil separation. Mater Res Express. 2019;6(10):105313. http://doi.org/10.1088/2053-1591/ab3754.

36. Amini M, Seifi M, Akbari A, Hosseinifard M. Polyamide-zinc oxide-based thin film nanocomposite membranes: towards improved performance for forward osmosis. Polyhedron. 2020;179:114362. http://doi.org/10.1016/j.poly.2020.114362.
37. Kowalik-Klimczak A, Woskowicz E, Kacprzyńska-Gołacka J. The surface modification of polyamide membranes using graphene oxide. Colloids Surf A Physicochem Eng Asp. 2020;587:124281. http://doi.org/10.1016/j.colsurfa.2019.124281.
38. Tang Q, Wang K, Ren X, Zhang Q, Lei W, Jiang T, et al. Preparation of porous antibacterial polyamide 6 (PA6) membrane with zinc oxide (ZnO) nanoparticles selectively localized at the pore walls via reactive extrusion. Sci Total Environ. 2020;715:137018. http://doi.org/10.1016/j.scitotenv.2020.137018. PMid:32041003.
39. Derakhshan Z, Ghaneian MT, Mahvi AH, Conti GO, Faramarzian M, Dehghani M, et al. A new recycling technique for the waste tires reuse. Environ Res. 2017;158:462-9. http://doi.org/10.1016/j.envres.2017.07.003.
40. Biron M. Recycling plastics: advantages and limitations of use. In: Biron M, editor. A practical guide to plastics sustainability: concept, solutions, and implementation. Norwich: William Andrew Publishing; 2020. p. 411-67. http://doi.org/10.1016/B978-0-12-821539-5.00009-4.
41. ASTM: American Society for Testing and Materials. ASTM F316-03: standard test methods for pore size characteristics of membrane filters by bubble point and mean flow pore test [Internet]. West Conshohocken: ASTM; 2014 [cited 2025 Jan 9]. Available from: http://www.astm.org/cgi-bin/resolver.cgi?F316-03(2011)
42. Bagheripour E, Moghadassi AR, Hosseini SM. Preparation and characterization of PES-Blend-Sulfonated PVC nanofiltration membranes: investigation of polymers blend ratio. Arabian J Sci Eng. 2016;41(7):2545-52. http://doi.org/10.1007/s13369-016-2026-5.
43. Chang H, Liang H, Qu F, Liu B, Yu H, Du X, et al. Hydraulic backwashing for low-pressure membranes in drinking water treatment: a review. J Memb Sci. 2017;540:362-80. http://doi.org/10.1016/j.memsci.2017.06.077.
44. Aguilar J, Rodríguez J, Hinojosa M. Microwaves as an energy source for producing β-SiC. J Microw Power Electromagn Energy. 2001;36(3):169-77. http://doi.org/10.1080/08327823.2001.11688458.
45. Wejrzanowski T, Tymicki E, Plocinski T, Bucki JJ, Tan TL. Design of SiC-doped piezoresistive pressure sensor for high-temperature applications. Sensors. 2021;21(18):6066. http://doi.org/10.3390/s21186066.
46. Halim NSA, Wirzal MDH, Bilad MR, Nordin NAHM, Putra ZA, Yusoff ARM, et al. Electrospun nylon 6,6/ZIF-8 nanofiber membrane for produced water filtration. Water. 2019;11(10):2111. http://doi.org/10.3390/w11102111.
47. Yan J, Nie L, Li G, Zhu Y, Gao M, Wu R, et al. Axial crystal growth evolution and crystallization characteristics of bi-continuous polyamide 66 membranes prepared via the cold non-solvent-induced phase separation technique. Polymers. 2022;14(9):1706. http://doi.org/10.3390/polym14091706.
48. Poletto P, Duarte J, Thürmer MB, Santos V, Zeni M. Characterization of polyamide 66 membranes prepared by phase inversion using formic acid and hydrochloric acid such as solvents. Mater Res. 2011;14(4):547-51. http://doi.org/10.1590/S1516-14392011005000087.
49. Jusoh WZAW, Rahman SA, Ahmad AL, Mokhtar NM. Fabrication and characterisation of a polyamide thin-film composite membrane on a nylon 6,6 substrate for isopropanol dehydration. C R Chim. 2019;22(11-12):755-60. http://doi.org/10.1016/j.crci.2019.08.001.
50. Chang HH, Chen SC, Lin DJ, Cheng LP. Preparation of bi-continuous Nylon-66 porous membranes by coagulation of incipient dopes in soft non-solvent baths. Desalination. 2013;313:77-86. http://doi.org/10.1016/j.desal.2012.12.009.
51. Elhady S, Bassyouni M, Mansour RA, Elzahar MH, Abdel-Hamid S, Elhenawy Y, et al. Oily wastewater treatment using polyamide thin film composite membrane technology. Membranes. 2020;10(5):1-17. http://doi.org/10.3390/membranes10050084.
52. Arahman N, Mulyati S, Lubis MR, Razi F, Takagi R, Matsuyama H. Modification of polyethersulfone hollow fiber membrane with different polymeric additives. Membr Water Treatment. 2016;7(4):355-65. http://doi.org/10.12989/mwt.2016.7.4.355.
53. Qaisrani TM, Samhaber WM. Impact of gas bubbling and backflushing on fouling control and membrane cleaning. Desalination. 2011;266(1-3):154-61. http://doi.org/10.1016/j.desal.2010.08.019.

Data Availability

The dataset supporting the results of this study is not publicly available.